J|A|C|S ARTICLES

Published on Web 03/17/2009

Direct Detection of Molecular Biorecognition by Dipole Sensing Mechanism

Ilya Goykhman,[†,‡] Nina Korbakov,[†] Carmen Bartic,[||] Gustaaf Borghs,[||] Micha E. Spira,[§] Joseph Shappir,[‡] and Shlomo Yitzchaik*[,†]

Institute of Chemistry, School of Engineering, Department of Neurobiology, The Hebrew University of Jerusalem, Safra Campus - Givat Ram, 91904, Jerusalem, Israel, and IMEC, MCP/ART, Cell Based Sensors & Circuits, Kapeldreef 75, 3001 Heverlee, Belgium

Received November 25, 2008; E-mail: sy@cc.huji.ac.il

Abstract: This work investigates the feasibility of transducing molecular-recognition events into a measurable potentiometric signal. It is shown for the first time that biorecognition of acetylcholine (ACh) can be translated to conformational changes in the enzyme, acetylcholine-esterase (AChE), which in turn induces a measurable change in surface potential. Our results show that a highly sensitive detector for ACh can be obtained by the dilute assembly of AChE on a floating gate derived field effect transistor (FG-FET). A wide concentration range response is observed for ACh (10^{-2}−10^{-9}M) and for the inhibitor carbamylcholine CCh (10^{-6}−10^{-11}M). These enhanced sensitivities are modeled theoretically and explained by the combined response of the device to local pH changes and molecular dipole variations due to the enzyme−substrate recognition event.

1. Introduction

Controlling and tuning the structural and electronic properties of semiconductor materials is one of the base concepts to technologically compatible realization of miniaturized devices. Of particular interest are the hybrid systems, in which integration of molecular functionalities to modify the established characteristics of devices provides a versatile tool to combine the synthetic diversity of the biochemical world with the robustness and scalability of modern semiconductor technology. The hybrid approach is based on adsorbing molecules or molecular layers onto the solid surface of the device to achieve control over the electrical or optical properties of the molecular−semiconductor interface. In this case the common way to "sense" the cooperative molecular events is to connect the transferred information to changes in electric potential rather than electronic transport through the molecules themselves.

In the past decade it was widely demonstrated that assembly of polar molecules onto bare semiconductors or metals strongly affects the electrical characteristics of the surface,[1−23] namely the external thin molecular layer on the order of a few nanometers which produces a pronounced effect on the work function and the barrier height of the interface.[1−10] For simplicity, the molecular tuning can be described in terms of modification of existing surface dipoles with the additional molecular dipole layer, which is identified by the change in effective electron affinity of the surface.[1−4,11−14] Theoretical and experimental works show that dipole size, orientation, and surface density[8−17] together with systematically varying dipole properties of the adsorbed molecules can lead to corresponding trends in the electrical characteristics of the

[†] Institute of Chemistry, The Hebrew University of Jerusalem.
[‡] School of Engineering, The Hebrew University of Jerusalem.
[§] Department of Neurobiology, The Hebrew University of Jerusalem.
[||] IMEC.

(1) Vilan, A.; Cahen, D. *Trends Biotechnol.* **2002**, *20*, 22–29.
(2) Haick, H.; Ambrico, M.; Ligonzo, T.; Tung, R. T.; Cahen, D. *J. Am. Chem. Soc.* **2006**, *128*, 6854–6869.
(3) Vilan, A.; Shanzer, A.; Cahen, D. *Nature (London)* **2000**, *404*, 166–168.
(4) Ashkenasy, G.; Cahen, D.; Cohen, R.; Shanzer, A.; Vilan, A. *Acc. Chem. Res.* **2002**, *35*, 121–128.
(5) Zuppiroli, L.; Si-Ahmed, L.; Kamaras, K.; Nüesch, F.; Bussac, M. N.; Ades, D.; Siove, A.; Moons, E.; Grätzel, M. *Eur. Phys J B* **1999**, *11*, 505.
(6) Crispin, X.; Geskin, V.; Crispin, A.; Cornil, J.; Lazzaroni, R.; Salaneck, W. R.; Bredas, J. L. *J. Am. Chem. Soc.* **2002**, *124*, 8131–8141.
(7) Deleted in proof.
(8) Krüger, J.; Bach, U.; Grätzel, M. *Adv. Mater.* **2000**, *12*, 447–451.
(9) Ofir, Y.; Zenou, N.; Goykhman, I.; Yitzchaik, S. *J. Phys. Chem. B* **2006**, *101*, 8002–8009.
(10) (a) Nüesch, F.; Rotzinger, F.; Si-Ahmed, L.; Zuppiroli, L *Chem. Phys. Lett.* **1998**, *288*, 861–867. (b) Ganzorig, C.; Kwak, K.-J.; Yagi, K.; Fujihira, M. *Appl. Phys. Lett.* **2001**, *79*, 272–274. (c) Rudich, Y.; Benjamin, I.; Naaman, R.; Thomas, E.; Trakhtenberg, S.; Ussyshkin, R *J. Phys. Chem. A* **2000**, *104*, 5238–5245. (d) Linford, M. R.; Fenter, P.; Eisenberger, P. M.; Chidsey, C. E. D. *J. Am. Chem. Soc.* **1995**, *117*, 3145–3155.
(11) Cohen, R.; Zenou, N.; Cahen, D.; Yitzchaik, S. *Chem. Phys. Lett.* **1997**, *279*, 270–274.
(12) Si-Ahmed, L.; Nüesch, F.; Zuppiroli, L.; Francüois, B. *Macromol. Chem. Phys.* **1998**, *199*, 625–632.
(13) Sfez, R.; Peor, N.; Cohen, S. R.; Cohen, H.; Yitzchaik, S *J. Mater. Chem.* **2006**, *16*, 4044–4050.
(14) Ray, S. G.; Cohen, H.; Naaman, R.; Liu, H.; Waldeck, D. H *J. Phys. Chem. B* **2005**, *109*, 14064–14073.
(15) Peor, N.; Sfez, R.; Yitzchaik, S. *J. Am. Chem. Soc.* **2008**, *130*, 4158–4165.
(16) Cohen, R.; Kronik, L.; Shanzer, A.; Cahen, D.; Liu, A.; Rosenwaks, Y.; Lorenz, J. K.; Ellis, A. B *J. Am. Chem. Soc.* **1999**, *121*, 10545–10553.
(17) Cohen, R.; Kronik, L.; Vilan, A.; Shanzer, A.; Rosenwaks, Y.; Cahen, D *Adv. Mater.* **2000**, *12*, 33–37.
(18) Cahen, D.; Kahn, A.; Umbach, E. *Mater. Today* **2005**, *8*, 32–41.
(19) Cui, Y.; Lieber, C. M. *Science* **2001**, *291*, 851–853.
(20) Ishii, H.; Sugiyama, K.; Ito, E.; Seki, K. *Adv. Mater.* **1999**, *11*, 605–625.

10.1021/ja809051p CCC: $40.75

molecular−semiconductor interface and the resulting device performance.[1−6,24−35] Recently, several studies were conducted regarding the depolarization effect and its influences on the packaging, ordering, and cluster size of the molecules.[14,36−39] In addition, the molecular tuning was indicated even in the case of oxide-bearing semiconductors[11−14,33,34,39,40] and further implementation of the idea in controlling the charge density of the conducting channel in configuration of field-effect transistor (FET). The use of molecules to regulate the surface properties is considered to be one of the major controlling factors in advanced chemical, bioelectronic, and optoelectronic sensors.

In this contribution we test polarizable biologically active molecules tailored to the concept of a bioelectronic sensing device and systematically examined whether the biomolecular recognition and receptor−analyte interactions can be sensed not only in terms of (biocatalytic) byproducts but also based on electrical and structural changes of the receptor itself, which are related to dipole tuning of the sensing area of the device. For this reason we used the well studied system of the enzyme acetylcholine esterase (AChE) and neurotransmitter acetylcholine (ACh). *In vivo* AChE resides within the cleft of the synaptic junction, and its typical attribute is the asymmetric spatial distribution of electric charges that generates one of the largest molecular dipoles (*ca.* 1200 D), oriented approximately along a deep, narrow gorge and pointing toward the catalytic site of the enzyme.[41−43] The AChE−ACh recognition is governed by electrostatic interactions, where the area of negative potential around the gorge entrance (peripheral sites) provides a binding locus for positively charged ACh, so that the enzyme dipole may guide the substrate toward the correct active site for further π−cation interaction.[44] In addition it was demonstrated that the formation of the AChE−ACh complex and resulting biocatalytic hydrolysis of ACh are accompanied by a large change of the enzyme conformation.[45−47] The above characteristics of the biological system led us to assume that AChE−ACh interactions influence the electric charge distribution of the immobilized enzyme, i.e., induces the changes of the receptor dipole properties in the vicinity of the coupling interface, and as a result should be detected with an underlying potentiometric transducer.

Employing active biomaterials in the sensors controlled by molecular recognition enables translating unique molecular properties into measurable electrical signals. We choose to realize this idea on the basis of ion sensitive field-effect transistors (ISFET), which provide a technologically and biologically compatible platform for bioelectronic integration. The ISFET (or additionally known as CHEMFET) is based on the FET configuration, but its gate is displaced into an electrolyte solution. This allows us to combine a potentiometric transducer (FET) with different bioreceptor types of various complexity, including either the biomolecular species (e.g., enzymes, antigens−antibodies, nucleic acids) or living biological systems (e.g., neurons, animal or plant cells, tissue slices).[48−54] Performing a potentiometric characterization assisted by amplification properties of the transistor assures a transduction of molecular biorecognition events with a significant improvement of the signal-to-noise ratio (SNR) especially in the detection of very low analyte concentrations. Simple on-chip integration of the ISFET sensor with an appropriate readout and signal processing circuits allows maintaining stable and accurate measurement, by minimizing and compensating for the undesirable effects such as temperature variations, drift of output signal, etc. The typical configuration of enzyme-modified ISFET (EnFET) involves a receptor's immobilization onto the exposed gate dielectric of the transistor, so the biological elements are retained in direct spatial contact with the electronic structure. In this configuration, the charge redistribution (or potential variation) at the bioelectronic coupling interface (transistor's gate) modifies the conductivity of the channel and therefore is transduced to the outgoing signal of current or voltage. In the present study we used the advanced configuration of the floating-gate EnFET,

(21) Saito, N.; Hayashi, K.; Sugimura, H.; Takai, O. *Langmuir* **2003**, *19*, 10632–10634.
(22) Reed, M. A.; Tour, J. M. *Appl. Phys. Lett.* **2000**, *77*, 1224.
(23) Iozzi, M. F.; Cossi, M. *J. Phys. Chem. B* **2005**, *109*, 15383–15390.
(24) Seker, F.; Meeker, K.; Kuech, T. F.; Ellis, A. B. *Chem. Rev.* **2000**, *100*, 2505–2536.
(25) Wu, D. G.; Ashkenasy, G.; Shvarts, D.; Ussyshkin, R. V.; Naaman, R.; Shanzer, A.; Cahen, D. *Angew. Chem. Int. Ed* **2000**, *39*, 4496–4500.
(26) Wu, D. G.; Cahen, D.; Graf, P.; Naaman, R.; Nitzan, A.; Shvarts, D. *Chem.s Eur. J* **2001**, *7*, 1743–1749.
(27) Cahen, D.; Naaman, R.; Vager, Z. *Adv. Funct. Mater.* **2005**, *15*, 1571–1578.
(28) Patolsky, F.; Zheng, G. F.; Lieber, C. M. *Anal. Chem.* **2006**, *78*, 4260–4269.
(29) Niwa, D.; Yamada, Y.; Homma, T.; Osaka, T. *J. Phys. Chem. B* **2004**, *108*, 3240–3245.
(30) Rampi, M. A.; Whitesides, G. M. *Chem. Phys.* **2002**, *281*, 373–391.
(31) Salomon, A.; Cahen, D.; Lindsay, S.; Tomfohr, J.; Engelkes, V. B.; Frisbie, C D. *Adv. Mater.* **2004**, *16*, 477.
(32) Shen, Y.; Hosseini, A. R.; Wong, M. H.; Malliaras, G. G *Chem. Phys. Chem.* **2004**, *5*, 16–25.
(33) Chabinyc, M. L.; Chen, X.; Holmlin, R. E.; Jacobs, H.; Skulason, H.; Frisbie, C D.; Mujica, V.; Ratner, M. A.; Rampi, M. A.; Whitesides, G. M. *J. Am. Chem. Soc.* **2002**, *124*, 11730–11736.
(34) Collier, C. P.; Wong, E. W.; Belohradsky, M.; Raymo, F. M.; Stoddart, J. F.; Kuekes, P. J.; Williams, R. S.; Heath, J. R. *Science* **1999**, *285*, 391–394.
(35) Liu, Y.; Yu, H. *Chem. Phys. Chem.* **2003**, *4*, 335–342.
(36) Kobayashi, T.; Nishikawa, T.; Takenobu, S.; Mori, T.; Shimoda, T.; Mitani, H.; Shimonati, N.; Yoshimoto, S.; Ogawa and Iwasa, Y *Nat. Mater.* **2004**, *3*, 317–322.
(37) He, T.; He, J.; Lu, M.; Chen, B.; Pang, H.; Reus, W. F.; Nolte, W. M.; Nackashi, D. P.; Franzon, P. D.; Tour, J. M *J. Am. Chem. Soc.* **2006**, *128*, 14537–14541.
(38) Deutsch, D.; Natan, A.; Shapira, Y.; Kronik, L. *J. Am. Chem. Soc.* **2007**, *129*, 2989–2997.
(39) Cornil, D.; Olivier, Y.; Geskin, V.; Cornil, J. *Adv. Funct. Mater.* **2007**, *17*, 1143–1148.
(40) Gershevitz, O.; Sukenik, C. N.; Ghabboun, J.; Cahen, D. *J. Am. Chem. Soc.* **2003**, *125*, 4730–4731.
(41) Gershewitz, O.; Grinstein, M.; Sukenik, C.; Regev, K.; Ghabboun, J.; Cahen, D *J. Phys. Chem. B* **2004**, *108*, 664–672.
(42) Porschke, D.; Créminon, C.; Cousin, X.; Bon, C.; Sussman, J. L.; Silman, I. *Biophys. J.* **1996**, *70*, 1603–1608.
(43) Felder, C. E.; Botti, S. A.; Lifson, S.; Silman, I.; Sussman, J. L. *J. Mol. Graphics Mod.* **1997**, *15*, 318–327.
(44) Botti, S. A.; Felder, C. E.; Sussman, J. L.; Silman, I. *Protein Eng.* **1998**, *11*, 415–420.
(45) Ripoll, D. R.; Faerman, C. H.; Axelsen, P. H.; Silman, I.; Sussman, J. L. *Proc. Natl. Acad. Sci. USA* **1993**, *90*, 5128–5132.
(46) Dziri, L.; Boussaad, S.; Tao, N.; Leblanc, R. M. *Langmuir* **1998**, *14*, 4853–4859.
(47) Celie, P.; Rossum-Fikkert, S.; van Dijk, W.; Brejc, K.; Smit, A.; Sixma, T *Neuron* **2004**, *41*, 907–914.
(48) Massoulie, J.; Pezzementi, L.; Bon, S.; Krejci, E.; Vallette, F. M. *Progress in Neurobiology* **1993**, *41*, 31–91.
(49) Bergveld, P.; Siabbald, A. *Analytical and Biomedical Applications of Ion-Selective Field Effect Transistor; Wilson and Wilson's Comprehensive Analytical Chemistry, Vol. 23*, Elsevier: Amsterdam 1988.
(50) Bergveld, P. *Sens. Actuators B* **2003**, *88*, 1–20.
(51) Schöning, M. J.; Poghossian, A. *Analyst* **2002**, *127*, 1137–1151.
(52) Janata, J. *Electroanalysis* **2004**, *16*, 1831–1835.
(53) Kharitonov, A. B.; Zayats, M.; Lichtenstein, A.; Katz, E.; Willner, I. *Sens. Actuators B* **2000**, *70*, 222–231.
(54) Cohen, A.; Spira, M. E.; Yitshaik, S.; Borghs, G.; Shwatzglass, O.; Shappir, J. *Biosens. Bioelec.* **2004**, *19*, 1703–1709.

Scheme 1. Stepwise Sssembly of AChE onto the Floating Gate Surface[a]

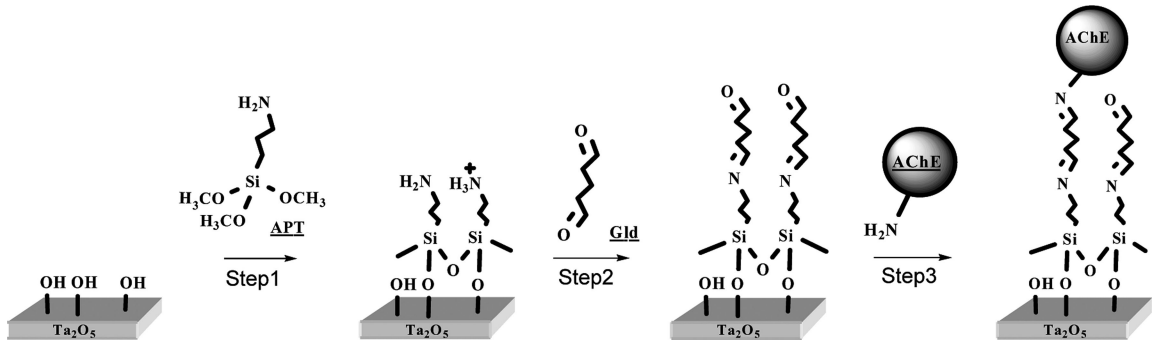

[a] Step 1: Primary modification of the Ta_2O_5 surface with APTES. Step 2: Activation of amino-functionalized region with glutaric dialdehyde. Step 3: Anchoring of the enzyme AChE.

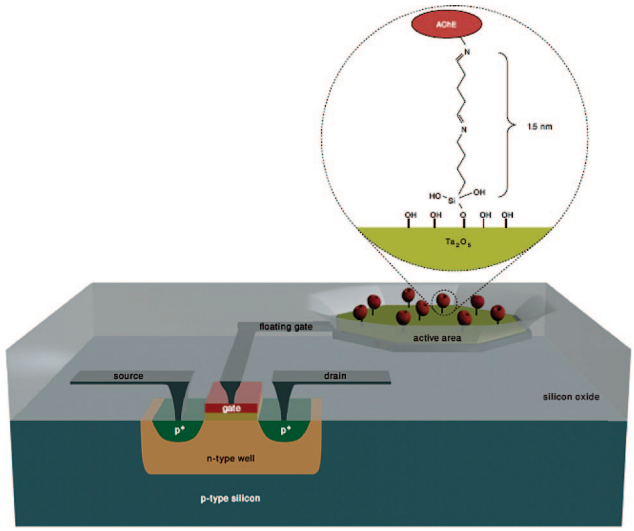

Figure 1. Floating-gate ISFET with AChE modified area.

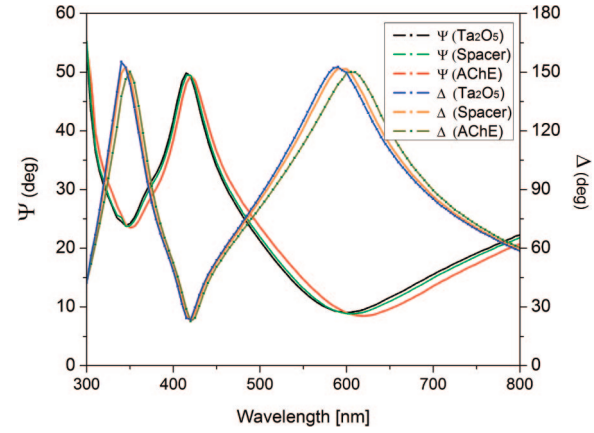

Figure 2. Representative spectroscopic ellipsometry measurement (for a single incidence angle, 75°) results recorded at each step of surface biochemical modification. Based on ellipsometric fitting results (see Supporting Information) the average thicknesses of spacer and AChE layers are 7.1 and 13.6 Å, respectively.

where the bioelectronic coupling area is shifted aside from the active transistor (Figure 1).

Previously, the floating-gate (FG) approach has been successfully tested in the realization of neuron-FET electrical coupling[53] and is found to be highly efficient for recording potential variations on the sensing surface. The implementation of FG in biosensor design offers several important advantages: (1) isolation and protection of the transistor from the ionic solution; (2) it enables increasing of sensing area without harming the response time of electronic system; (3) it allows improving of system sensitivity by increasing FG to channel area ratio; (4) and the most important for our purpose is that the floating electrode in fact "integrates" the local charge variations (e.g., discrete events) into a total representative signal, which uniformly modulates the transistor channel potential.

During the molecular grafting we tried to emphasize several considerations. First, to improve the coupling efficiency between enzyme dipole characteristics and the sensing area, the active molecules were immobilized within the dimension of a double layer (*ca.* a few nanometers in a physiological-type solution) to avoid the shielding effect of the counterions from solution.[50] In addition, our previous experience shows that the aromatic spacer also gives rise to the shielding factor and diminishes the transduction efficiency.[14] Therefore, we choose the aliphatic spacer to anchor the AChE to the surface. Finally, we were not concerned with the assembly of a perfect, highly ordered layer of AChE in minimizing the depolarization effect due to intermolecular dipole−dipole interactions within the enzyme layer. In contrast, we took advantage of the large FG area to carry out the diluted surface coverage, relying on integrating the effect of the floating electrode. For these reasons, the biomaterial grafting was realized first by surface modification with the submonolayer density of 3-aminopropyltrimethoxysilane (APTES), followed by a covalent binding of AChE via the molecular bridge of glutaric dialdehyde; see Scheme 1. The assembly of the enzyme layer was verified by X-ray photoelectron spectroscopy (XPS), and partial surface coverage was deduced from variable angle spectroscopic ellipsometry (VASE) characterization, presented in Figure 2. The activity of the immobilized enzyme was confirmed by kinetic measurements[54,55] and by the Karnovski and Root dyeing method[56] (see Supporting Information).

2. Experimental Section

2.1. Fabrication. The floating gate p-channel transistors were realized in a standard 0.18 μm CMOS process with modification of the channel implant to obtain depletion type devices. A 1000 Å thick tantalum pentoxide layer was sputtered over an exposed aluminum pad, which was connected to the polycrystalline-silicon

(55) Hai, A.; Ben-Haim, D.; Korbakov, N.; Cohen, A.; Shappir, J.; Oren, R.; Spira, M. E.; Yitzchaik, S. *Biosens. Bioelec.* **2006**, *22*, 605–612.
(56) Ellman, G. L.; Courtney, K. D.; Andres, V.; Featherstone, R. M. *Biochem. Pharmacol.* **1961**, *7*, 88–95.

gate, to obtain a floating electrode with high capacitive coupling to the solution.

Following a microelectronic fabrication process the completed wafer was cut by a diamond saw to individual dies. After cleaning in ethanol, the dies were packaged in dual in-line (DIL) socket with 28 pins and connected with a 25 μm thick gold wire by a bonding machine (KS model 4522). The exposed metal connections that are found around a chip periphery were insulated with highly thixotropic epoxy with nonflowing properties (EPO-TEK 353ND-T), so that the central part of the silicon die, where the floating gate electrodes are located, remained exposed and available for further biochemical modifications. To achieve good adhesion between the silicon die and epoxy, the encapsulation procedure was performed under low humidity ambient conditions (<43%) during continuous chip heating at 100 °C.

2.2. Biochemical Modification. All the chemicals and reagents used in this work were purchased from Sigma-Aldrich. APTES, 3-aminopropyltrimethoxysilane, was vacuum distilled prior to its use. For primary modification a solution of 4 μL of APTES in methanol (0.4% v/v) was applied for 15 min at room temperature (RT) to the Ta_2O_5 floating gate surface. Afterward the chip was thoroughly rinsed in the same solvent three times and dried for 30 min in air. The propylamine functionalized area was activated for 30 min at RT with an aqueous solution consisting of 1% (w/w) glutaric dialdehyde and triple distilled water (TDW, 18.3 MΩ•cm). Following same cleaning procedure the modified area was immersed for 1 h in the AChE (from human source) solution, which was prepared by adding 1 mL of PBS (0.1 M KH_2PO_4, 0.1 M NaOH, pH 7.4) to 0.1 mg of lyophilized AChE in powder form (stocked at 4 °C).

2.3. Surface Analysis. Silicon substrates with Ta_2O_5 sputtered layer were used to imitate the floating gate surface at each step of chemical modification. First, the samples were sonicated in 0.2% (v/v) soapy water at 60 °C, thoroughly washed with triple distilled water (TDW), and then dipped in hot (90 °C) piranha solution for 60 min (3:7 by volume of 30% H_2O_2 (MOS) and concd H_2SO_4 (MOS "BAK-ANAL" REAG) (*Caution:* strong oxidizing solution, handle with care). Afterward, substrates were rinsed with TDW and further cleaned with $H_2O/H_2O_2/NH_3$ (5:1:0.25) solution while sonicating for 15 min at 60 °C. After subsequent washing with TDW, the substrates were dried under a stream of nitrogen. Following biochemical modification the XPS spectra were collected at ultrahigh vacuum (2.5×10^{-10}Torr) on a 5600 Multi-Technique (AES/XPS) system (PHI) using an X-ray source of Al K (1486.6 eV). VASE measurements were carried out on a VB-200 spectroscopic ellipsometer (Woollam Co.). AChE activity was assayed using UV−vis spectroscopy according to the basic procedure described in ref 55 acquired on a Shimadzu UV-3101PC spectrophotometer.

Enzyme assembly to the surface was verified by X-ray photoelectron spectroscopy (XPS) by the 8% decrease in the Ta $4f_{7/2}$ and Ta $4f_{5/2}$ (BE = 27.3 and 29.2 eV) signals and the appearance of the N 1s (BE = 401.69 eV) signal. Surface coverage was deduced from variable angle spectroscopic ellipsometry (VASE) characterizations. The ellipsometric data were acquired at three angles of incident (namely, 72°, 75°, and 78°) resulting in an average thickness of the AChE layer on order of 13.6 ± 0.7 Å (see also SF 1, Supporting Information). Taking into account the dimensions of AChE (6.5 nm × 6.0 nm × 4.5 nm) we estimated an average surface coverage of ~20%. The activity of immobilized enzyme was confirmed by kinetic measurements[54,55] where AChE-modified substrates were inserted into a PBS solution with acetylthiocholine iodide (ATChI, homologue of ACh) and indicator DTNB (5,5-dithio-bis(2-nitro-benzoic acid)). The final product of ATChI enzymatic hydrolysis, thiocholine, reacts with the DTNB indicator to give the yellow colored TNB (5,5-dithio-bis(2-nitrobenzoate)) anion, of which the concentration was monitored photometrically at 412 nm in situ in real time. The obtained increase in optical density and saturation indicated that immobilized AChE preserves its biocatalytic activity (see SF 2a, Supporting Information). Moreover, the activity of the anchored enzyme was verified by the Karnovsky and Roots dyeing method,[56] where a qualitative indication is obtained by the formation of brown precipitate that can be observed by optical microscopy (see SF 2b, Supporting Information). In short, this method uses ATChI in a phosphate buffer (PB) solution at pH 6 in an aqueous dyeing solution composed of sodium citrate, $CuSO_4$, and potassium ferricyanide. Thiocholine, the biocatalytic product, reduces the ferricyanide to ferrocyanide. The copper(II) ion reacts with ferrocyanide to yield the precipitate, a cupric ferrocyanide complex—Hatchett's brown.

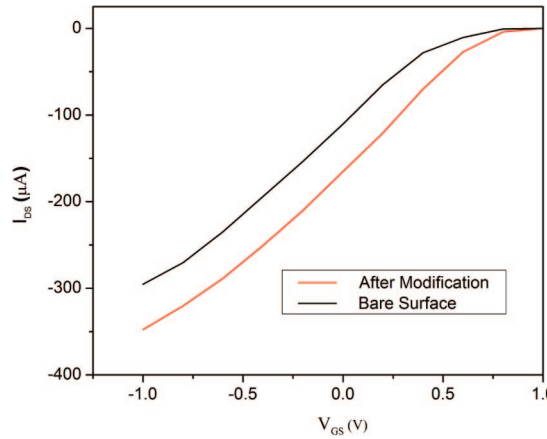

Figure 3. FG ISFET characteristics before and after biochemical modification ($V_{DS} = -0.1$ V).

2.4. Electrical Measurements. All electrical measurements were performed at room temperature in a custom-built liquid cell with a phosphate buffer saline (PBS) solution (background electrolyte pH 7.4), when a standard Ag/AgCl electrode was used as the reference electrode. The electrical characteristics of the systems were carried out with Keithley 237 source-measurement units, where the signals were recorded using a LabView-program interface.

3. Results and Discussion

The character of AChE−ACh interactions involve the catalyzed hydrolysis of ACh by AChE, resulting in acetic acid formation (the byproduct) in the vicinity of the sensing surface. So far, in the case of ACh potentiometric measurements, the detection mechanism was mainly attributed to proton adsorption (pH-sensing)[50,52,54] and described in terms of surface hydroxides equilibrium with the environment according to site-dissociation theory.[48] Therefore, as a first step we tested the pH-sensitivity of the nonfunctionalized device and estimated its value at room temperature as *ca.* 58.5 mV/pH, close to the ideal Nernstian response 59.2 mV/pH.[48] To confirm the fact that after AChE immobilization the external dipoles affect the device characteristics, we performed $I-V$ measurements before and after surface modification with AChE. Our results show clearly (Figure 3) that surface immobilization of enzyme causes a severe change of the device operation point compared to the bare transistor.

Figure 4a represents the electrical measurements of the AChE-modified device for different ACh concentrations, where the enzymatic activity is indicated as the definite shifts between the $I-V$ curves. Figure 4b concludes the dose responses of functionalized system and the control device, which has not undergone the AChE immobilization.

According to Figure 4b one can see that, in the case of the enzyme-modified device, there is a well-defined effect of potential alternation across the sensing surface. The obtained

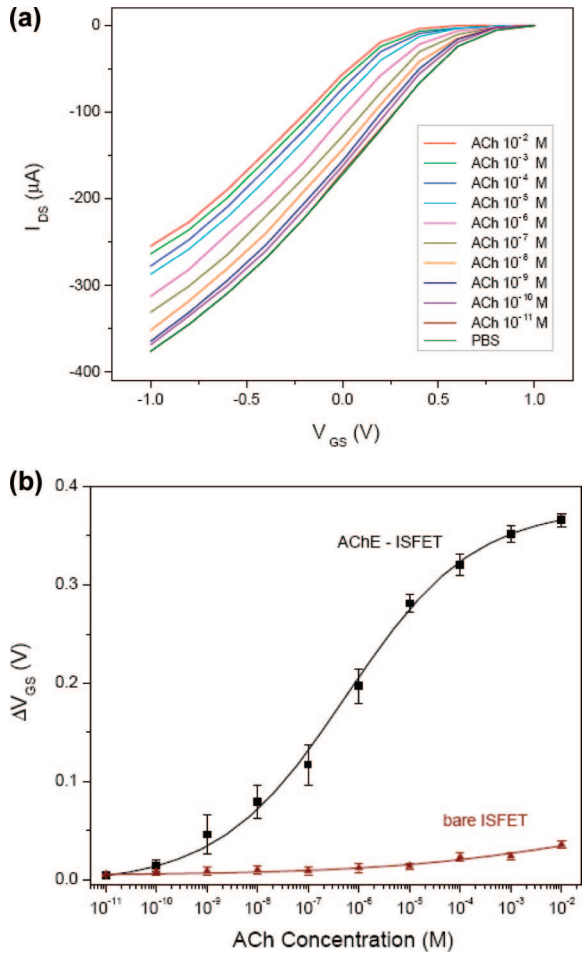

Figure 4. (a) EnFET sensitivity to different ACh concentration (transfer characteristics, $V_{DS} = -0.1$ V). (b) Dose response plot of EnFET and nonmodified control ISFET as derived from the transfer characteristics. The error bars represent the standard deviation in seven independent experiments.

sigmoid-shaped curve comes in full agreement with standard properties of surface reactions and normal enzyme kinetics. In contrast to the nonfunctionalized transistor, the hybrid system reveals a clear response to a wide range of ACh concentrations ($10^{-2}-10^{-10}$ M). The modest response generated by a control device to substrate concentrations higher than 10^{-4} M is attributed to the ACh equilibrium state and affinity toward the surface.

Based on the dose response results of the functionalized transistor (Figure 4b), the application of ACh is accompanied by a gate voltage shift of ~360 mV (derived as a difference in threshold voltage between a measurement result in PBS and dose response to ACh application of 10^{-2} M). Nevertheless, if in the present case the whole range of surface potential variation is ascribed only to proton adsorption (pH-sensing), then according to the pH-sensitivity of the bare device (*ca.* 58.5 mV/pH) one may calculate that the enzymatic activity produces almost 6 orders of magnitude of pH-variation near the sensing area. Taking into account the diluted assembly of AChE and enzyme fast degradation at low pH, together with routine products diffusing away from the active area, the aforementioned wide range response to ~6 orders of magnitude of ACh concentration seems to be hardly acceptable only in terms of pH-sensing.

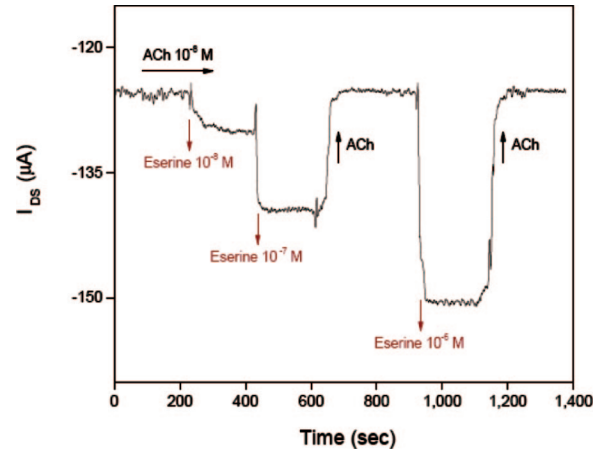

Figure 5. EnFET sensitivity to eserine: Application of different doses of eserine inhibits enzymatic activity and brings about variation of device operation point. Elimination of eserine from electrolyte solution ($t = 600$ s, 1100 s) shows the reconstruction of initial reference signal.

To validate the fact that after immobilization and throughout the electrical measurements the enzyme preserves its normal pharmacological properties, we have recorded the EnFET response to eserine, a competitive and reversible inhibitor of AChE.[57] Figure 5 demonstrates an output current monitoring of the enzyme-modified system during eserine applications.

As it is shown, ACh at concentration 10^{-8} M is used to produce a reference signal. The application of an increased dose of eserine ($10^{-8}-10^{-6}$ M) inhibits the enzymatic activity and effectively decries the proton concentration near the sensing area. As a result the outgoing current varies (effectively increases) and matches itself to the new surface conditions. To check process reversibility we performed a complete removal of eserine from the reaction medium by continuous injection of buffer solution with a constant ACh concentration of 10^{-8} M (see Figure 5 at time 600 s and 1100 s). The time response data show clearly that eserine elimination from the system led to full reconstruction of the initial level of the current. Combining these observations together with approved stability tests, we could state that the variations of the device operation point were related to the presence and activity of the enzyme.

Relying on the previous observations we examined whether the AChE-based sensor can detect a nonhydrolyzable ACh agonist carbamylcholine (CCh); see Figure 6. The structure similarity between ACh and CCh together with the fact that carbamylcholine does not undergo hydrolysis by AChE excludes the contribution of proton adsorption to the total surface potential variation. We noticed that also in the case of CCh the hybrid system produces a well-defined profile of the dose response. We think that in the present situation the device sensitivity and dose response to CCh are wholly related to the binding events and ensuing enzyme conformation changes that contribute to the dipole variations at the bioelectronic interface.

Our interpretation is greatly supported by the construction of a theoretical model, considering the net alteration in surface potential (ΔV_{GS}) due to parallel effects of (a) pH-changes adjacent to the sensing area (so-called pH-mechanism, mainly governed by the byproducts formation) and (b) induced variations of the enzyme dipole layer (dipole mechanism, related to

(57) Karnovsky, M. J.; Roots, L. *J. Histochem. Cytochem.* **1964**, *12*, 219.

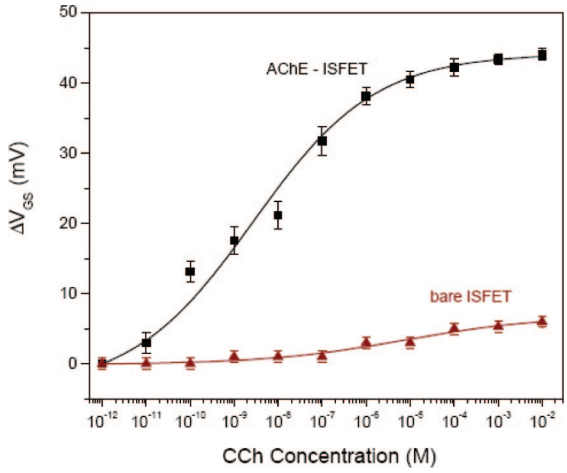

Figure 6. Dose response curves of AChE-functionalized and nonmodified devices to carbamylcholine. The error bars represent the standard deviation in four independent experiments.

the properties of the receptor). The pH-dependent contribution is deduced from the site-dissociation theory[48] and is given by

$$\Delta\Psi(S) = 2.303\frac{k_B T}{q} \cdot \alpha \cdot (\mathrm{pH}_{pzc} - \Delta\mathrm{pH}(S)) \qquad (1)$$

where $\Delta\Psi(S)$ is the surface potential change induced by the specific concentration of substrate and related to pH (S is the substrate concentration, e.g., ACh), $2.303 \cdot k_B T/q$ is the ideal Nernstian response, α is the sensitivity parameter ($0 < \alpha < 1$), pH_{pzc} is the pH at the potential of zero charge, and $\Delta\mathrm{pH}(S)$ is the pH variation near the sensing surface as a result of enzymatic activity.

The portion of dipole variations is described according to the Helmholtz relation:[1]

$$\Delta\varphi(S) = \frac{N(S) \cdot \Delta\mu \cdot \cos\theta}{\varepsilon\varepsilon_0} \qquad (2)$$

where $\Delta\varphi(S)$ is the surface potential change induced by the specific concentration of the substrate and related to the dipole, $N(S)$ is the surface density of the enzyme−substrate complex, $\Delta\mu$ describes the average dipole change in receptor due to interaction with an analyte (in debye), θ is the average dipole angle with respect to the surface normal, ε is the effective dielectric constant of the molecular film, and ε_0 is the permittivity of vacuum. It is worth noting here that an enzyme−substrate reaction is a saturable process. Therefore, the change of complex density $N(S)$ is suited to enzyme kinetics and is described according to the Michaelis−Menten model of single substrate reactions. As a result,

$$N(S) = \frac{N_0}{1 + (k_M/S)^{2/3}} \qquad (3)$$

where N_0 is the enzyme's surface density (number of enzymes per unit area), k_M is the Michaelis−Menten constant, 2/3 is the scaling factor from 3D to 2D system, and S is the substrate concentration. Finally, the total variation of surface potential due to the presence of a particular substrate is given by [see also, Supporting Information]

$$\Delta V(S) = \Delta\Psi(S) + \Delta\varphi(S) \qquad (4)$$

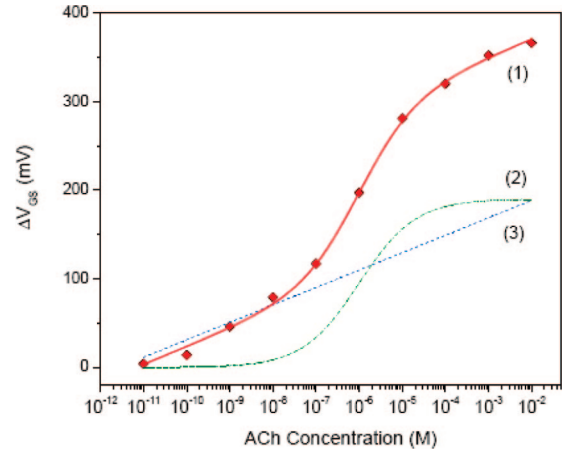

Figure 7. Results of fit simulation between the theoretical model (red line) and the experimental data (red diamonds) of dose response to ACh. (1) The combined pH and dipole detection mechanisms. (2) Dipole-mechanism alone. (3) pH-mechanism alone.

Table 1. Comparison between the Simulation Results and the Physical Values Obtained from the Experiment or Literature

fitting parameter	simulated value	physical value	reference's agreement
$2.303 \cdot (k_B T)/(q) \cdot \alpha$	58×10^{-3} V	58.5×10^{-3} V	experimental data
pH_{pzc}	4.1	3−6.5	58
k_d	7×10^{-5} M	5.4×10^{-5} M	59
ε	3.7	4	60
k_M	2×10^{-6} M	4.6×10^{-5}−10^{-4} M	61−63

Figure 7 represents the fit between the simulation of the theoretical model and the experimental data of the dose response to ACh (Figure 4b).

The simulated curve demonstrates good agreement with the experiment. In addition, the correspondence of fitting parameters [see also, Supporting Information] to the literature is summarized in Table 1.

According to the simulation, neither pH nor dipole mechanism can describe separately the dose response curve of the AChE-modified device, and only the combination of the two factors that modulate the surface potential (pH and dipole) introduce a qualitative agreement to experimental results (Figure 6). Based on simulation, the contribution of each process was ∼186 and 181 mV for pH and dipole mechanisms, respectively, and the derived AChE dipole change during interaction with ACh is *ca.* 280 D, which is ∼20% of the AChE dipole.

4. Conclusions

In contrast to macro-biomolecular recognition (*e.g.*, antigen−antibody) based on changes in the layer's dielectric properties, this work demonstrates for the first time that

(58) Changeux, J.; Leuzinger, W.; Huchet, M. *FEBS Lett.* **1968**, *2*, 77–80.
(59) Kosmulski, M. *Langmuir* **1997**, *13*, 6315–6320.
(60) Bourne, Y.; Radic, Z.; Sulzenbacher, G.; Kim, E.; Taylor, P.; Marchot, P. *J. Biol. Chem.* **2006**, *281*, 29256–29267.
(61) Wlodek, S. T.; Shen, T.; McCammon, J. A. *Biopolymers* **2000**, *53*, 265–271.
(62) Kronman, C.; Ordentlich, A.; Barak, B.; Velan, B.; Shaffermanf, A. *J. Biol. Chem.* **1994**, *269*, 27819–27822.
(63) Selwood, T.; Feaster, S. R.; States, M. J.; Pryor, A. N.; Quinn, D. M. *J. Am. Chem. Soc.* **1993**, *115*, 10477–10482.
(64) Radic, Z.; Pickering, N. A.; Vellom, D. C.; Camp, S.; Taylor, P. *Biochemistry* **1993**, *32*, 12074–12084.

biorecognition of the small biomolecules can be translated to conformational changes in the bioreceptor that in turn induces a measurable change in surface potential. Our results show clearly that a polarizable receptor can tune the electrical properties of the potentiometric device only by its dipole effect. The ability to characterize biomolecular interaction based upon the dipole properties of the receptor shows a direct way to translate the biomolecular-recognition event, rather than indirect characterization according to the interaction's biocatalytic byproducts. In principle, any biomolecular recognition event (enzyme−substrate/inhibitors, receptor−neurotransmitter/hormones, *etc*.) that is accompanied by dipole changes may be detected by this method.

Acknowledgment. The project is funded by the European Union Sixth Program IST-510574 (Golden Brain) and initiated by an FET grant of the fifth Programme IST-1999-29091.

Supporting Information Available: VASE measurement results and fitting, AChE activity results, the design of microelectronic structure, FG ISFET pH characteristics, and description of analytical model. This material is available free of charge via the Internet at http://pubs.acs.org.

JA809051P